Brazilian Journal
of Chemical
Engineering

ISSN 0104-6632
Printed in Brazil
www.abeq.org.br/bjche

Vol. 33, No. 01, pp. 91 - 104, January - March, 2016
dx.doi.org/10.1590/0104-6632.20160331s20150530

MODELING AND ANALYSIS OF UNSTEADY FLOW BEHAVIOR IN DEEPWATER CONTROLLED MUD-CAP DRILLING

Jiwei Li[1*], Gonghui Liu[1,2], Jun Li[1] and Mengbo Li[1,3]

[1]China University of Petroleum, College of Petroleum Engineering, Beijing 102249, China.
Phone: + 86 010 89731225
E-mail: lijiwei2009@live.com
[2]Beijing University of Technology, Beijing 100192, China.
[3]China National Offshore Oil Corporation Research Institute, Beijing 100010, China.

(Submitted: August 24, 2015 ; Revised: November 13, 2015 ; Accepted: November 30, 2015)

Abstract - A new mathematical model was developed in this study to simulate the unsteady flow in controlled mud-cap drilling systems. The model can predict the time-dependent flow inside the drill string and annulus after a circulation break. This model consists of the continuity and momentum equations solved using the explicit Euler method. The model considers both Newtonian and non-Newtonian fluids flowing inside the drill string and annular space. The model predicts the transient flow velocity of mud, the equilibrium time, and the change in the bottom hole pressure (BHP) during the unsteady flow. The model was verified using data from U-tube flow experiments reported in the literature. The result shows that the model is accurate, with a maximum average error of 3.56% for the velocity prediction. Together with the measured data, the computed transient flow behavior can be used to better detect well kick and a loss of circulation after the mud pump is shut down. The model sensitivity analysis show that the water depth, mud density and drill string size are the three major factors affecting the fluctuation of the BHP after a circulation break. These factors should be carefully examined in well design and drilling operations to minimize BHP fluctuation and well kick. This study provides the fundamentals for designing a safe system in controlled mud-cap drilling operatio.
Keyword: Deep water; Controlled mud-cap drilling; Unsteady flow; Mathematical model; Kick detection.

INTRODUCTION

Due to the depletion of onshore oil and gas resources, the oil-gas industry has extended its search for resources to deep-water areas. However, deep-water drilling is facing many problems and challenges, including pore pressure prediction uncertainties, narrow pressure margins, and high equivalent circulation density (ECD) (Shaughnessy *et al*., 1999; 2007; Stave, 2014). These problems and challenges not only lead to the inability to design wells for traditional kick tolerances, but also make a well technically undrillable due to lack of drilling window right below the previous casing/liner shoe. Controlled mud cap (CMC) drilling is the solution to all of these problems and challenges, and improve safety and efficiency in the well construction process (JPT staff, 2013; Stave, 2014; Malt and Stave, 2014; Godhavn *et al*, 2014; Børre and Sigbjørn, 2014).

CMC drilling is a kind of subsea mud-lift pump drilling system technologies. Figure 1 shows a schematic of a CMC drilling system. The mud-lift pump is placed in water and return mud and cuttings to surface through a mud return line (MRL). The technique allows for precise control of bottom hole pressure (BHP) during drilling by regulating the mud

*To whom correspondence should be addressed

level in the marine riser. This method can improve the safety margins and drill longer open hole sections in wells with narrow operational mud windows (Børre and Sigbjørn, 2006).

Furthermore, the mud level in the annulus is positioned below the mud level inside the drill string during CMC drilling but not conventional drilling. Therefore, there is a potential pressure imbalance between the fluids in the drill string and the annulus. After surface pump is shut down, the mud in the drill string will continue to flow downwards along the drill string, through the drill bit, and upwards along the annulus until an equilibrium between the mud column pressures in the drill string and annulus is reached. This process constitutes an unsteady flow (Choe *et al*., 1998; 1999; 2007).

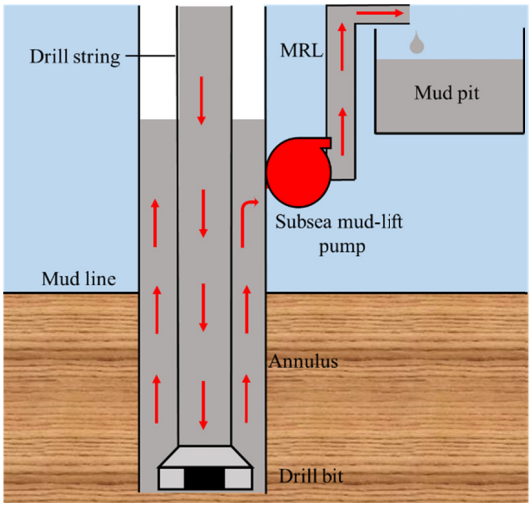

Figure 1: Schematic of the CMC drilling system.

After a circulation break, the uncontrolled unsteady flow can cause a significant problem during drilling in CMC drilling, especially in deepwater narrow-margin formations. During the unsteady flow, the mud will flow into the annulus from the drill string due to pressure imbalance between the drill string and the annulus. The increase in the mud level in the riser may cause an increase in the BHP, which may lead to a loss of circulation; the disappearance of the friction pressure loss can reduce the BHP, resulting in kick. Drill string valves (DSVs) can be used to solve these problems (Schubert and Juvkam-world, 2006), but this additional device is currently not very reliable. Moreover, DSVs can bring additional restrictions to drilling operations. Therefore, the effect of unsteady flow on the BHP must be known. However, we have not found any sufficient model in literatures to address this issue, which has motivated us to investigate into the problem.

The unsteady flow has always been a practical challenge for operations, such as the pumping of heavy mud of cementing (Sauer, 1987). For CMC drilling, unsteady flow is also a potential problem in common operations, such as the connection, tripping and disconnection of the drill string. In 2007, Choe and co-workers presented a simple formula describing the unsteady flow for a subsea mud-lift drilling (SMD) system (Choe, 2007), but they did not carry out a detailed theoretical analysis and verification. Moreover, CMC drilling is different from SMD, and the formula describing unsteady flow for SMD is not suitable for CMC drilling.

A few studies have examined the unsteady flow after a circulation break. However, a detailed simulation study of the transient change in the BHP during the unsteady flow has not been published yet. Kick detection methods for CMC drilling systems after a circulation break are scarce. In this study, a new mathematical model describing the unsteady flow after surface pump shutting down for CMC drilling is developed and validated with experiment from the literature (Ogawa *et al*., 2007). A numerical simulation based on the explicit Euler was performed to investigate the transient behaviors of mudflow velocity, mud level in the annulus and BHP. This paper presents an accurate detection method for the kick and loss of circulation after a circulation break. Sensitivity analysis was performed to better understand the effects of system parameters on transient flow behaviors during unsteady flow. This study provides the fundamentals for designing a safe system for controlled mud-cap drilling operations.

MATHEMATICAL MODEL

Governing Equation

The governing equation for the liquid flow velocity in the annulus is derived in Appendix A. The resultant form is

$$\frac{\partial U_{Ann}}{\partial t} = -\frac{U_{Ann}^2 - U_{DC}^2}{2(L_{Ann} + \frac{A_{Ann}}{A_{DC}} L_{DC})} - \frac{P_{DC,0} - P_{Ann,0}}{\rho(L_{Ann} + \frac{A_{Ann}}{A_{DC}} L_{DC})} - \frac{P_{f,DC} + P_{f,Ann} + P_{bit}}{\rho(L_{Ann} + \frac{A_{Ann}}{A_{DC}} L_{DC})} + \frac{(L_{DC} - L_{Ann})g}{(L_{Ann} + \frac{A_{Ann}}{A_{DC}} L_{DC})} \quad (1)$$

The first right-hand side term is the kinetic velocity due to the difference in the cross-sectional area between the drill string and the annulus. The second

right-hand side term takes into account the boundary pressure at the mud level in the drill string and the annulus. The third right-hand side term is related to friction, and the last right-hand side term represents the driving mechanism caused by the hydrostatic pressure imbalance between the drill string and the annulus. All symbols are defined in the Nomenclature section.

The final expression for the equation of motion for the length of mud, L_{Ann}, in the annulus is obtained:

$$\frac{\partial L_{Ann}}{\partial t} = -U_{Ann} \tag{2}$$

These two equations are solved numerically in a computer program.

Numerical Formulation

Because the mud level is not changing very rapidly, the numerical integration need not to be excessive. The explicit Euler method is locally second-order accurate but first-order globally accurate (Bewley, 2012). Provided that the time step is small enough, the explicit Euler method will yield good results for the problem. The simplest and most intuitive way of integrating the above scheme is by using the explicit Euler method, which takes the following form for Equation (1):

$$\begin{aligned} U_{Ann}^{n+1} = U_{Ann}^{n} - \Delta t \times \Bigg[& \frac{U_{Ann}^{n} U_{Ann}^{n} - U_{DC}^{n} U_{DC}^{n}}{2(L_{Ann}^{n} + \frac{A_{Ann}}{A_{DC}} L_{DC}^{n})} - \\ & - \frac{P_{DC,0}^{n} - P_{Ann,0}^{n}}{\rho(L_{Ann}^{n} + \frac{A_{Ann}}{A_{DC}} L_{DC}^{n})} - \\ & - \frac{P_{f,DC}^{n} + P_{f,Ann}^{n} + P_{bit}^{n}}{\rho(L_{Ann}^{n} + \frac{A_{Ann}}{A_{DC}} L_{DC}^{n})} + \\ & + \frac{g(L_{DC}^{n} - L_{Ann}^{n})}{(L_{Ann}^{n} + \frac{A_{Ann}}{A_{DC}} L_{DC}^{n})} \Bigg] \end{aligned} \tag{3}$$

The explicit scheme of the length of the mud column in annulus is

$$L_{Ann}^{n+1} = L_{Ann}^{n} + U_{Ann}^{n+1} \Delta t \tag{4}$$

Eq. (3) can be easily solved using the velocity and position of the previous time step to solve for the acceleration of mud in annulus in each time step. The acceleration is then used to obtain the velocity of mud in annulus, which in turn is used to calculate the position of the liquid level in annulus. In practice, the routine can be summarized as follows:

- Use Eq. (3) to update the acceleration based on the level position and velocity at the previous time step;
- Use Eq. (4) to update the level position based on the new velocity.

This procedure is repeated for each time step until the maximum time is reached.

Initial Conditions

After a circulation break, the initial mudflow velocity in the drill string is equal to that in the string before a circulation break:

$$U_{DC}(t=0) = U_0 \tag{5}$$

During normal circulation, the length of the mud column within the drill string is equal to the well depth:

$$L_{DC}(t=0) = L_{well} \tag{6}$$

The annulus pressure at subsea level is approximately equal to the seawater hydrostatic pressure; therefore, the length of the mud column within the annulus can be calculated using the following equation:

$$L_{ann}(t=0) = L_{well} - \frac{\rho - \rho_w}{\rho} h_w \tag{7}$$

RESULT AND ANALYSIS

Model Verification

Field experimental test for the unsteady flow after a circulation break are not currently available for a CMC drilling system. In 2007, Akira Ogawa *et al*. studied the flow in a U-tube in a laboratory (Ogawa *et al*, 2007). They adopted 3 non-Newtonian fluids to carry unsteady flow experiments in a U-tube: 68% glycerin solution, 1.8% acrylic co-polymer solution

and 3% acrylic co-polymer solution. The experimental device is shown in Figure 2. The inner diameter (ID) of the U- tube is 40 mm. During the experiment, high-speed cameras were used to record the experimental procedure. The data from the 3 non-Newtonian fluid flow experiments were used in this study to validate the developed unsteady flow mathematical model. The values of the specific experimental parameters are shown in Table 1.

Figures 3-5 show the comparisons of the recorded experimental results and the calculated results for 3 different non-Newtonian fluids. Both the flow velocities and the fluid level data agree well for the 3 non-Newtonian fluids. The errors are shown in Table 2, indicating the maximum average error of the flow velocity is 3.56%, which is within the allowable range of the engineering applications. The error is partially due to neglecting the capillary effect in the model. The scale of the experiment apparatus is small, and the capillary effect can be significant, whereas the capillary effect has not been taken into consideration in the mathematical model.

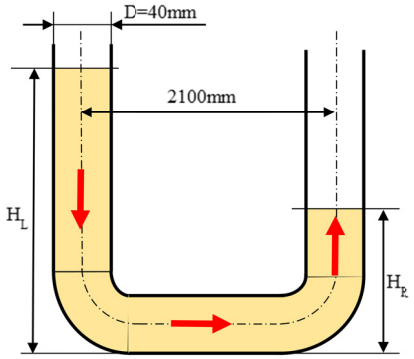

Figure 2: Schematic illustration of the experimental apparatus.

Table 1: Parameter values in the unsteady flow experiments.

Fluid Type	Left-liquid height H_L	Right-liquid height H_R	Balanced liquid surface height	Density	Dynamic viscosity	Kinematic viscosity
68% glycerin solution	870 mm	670 mm	770 mm	1200 kg/m^3	20.76×10^{-3} Pa·s	173×10^{-6} m^2/s
1.8% acrylic co-polymer	870 mm	670 mm	770 mm	1030 kg/m^3	17.4×10^{-3} Pa·s	169×10^{-6} m^2/s
3% acrylic co-polymer	870 mm	670 mm	770 mm	1030 kg/m^3	41.8×10^{-3} Pa·s	40.4×10^{-6} m^2/s

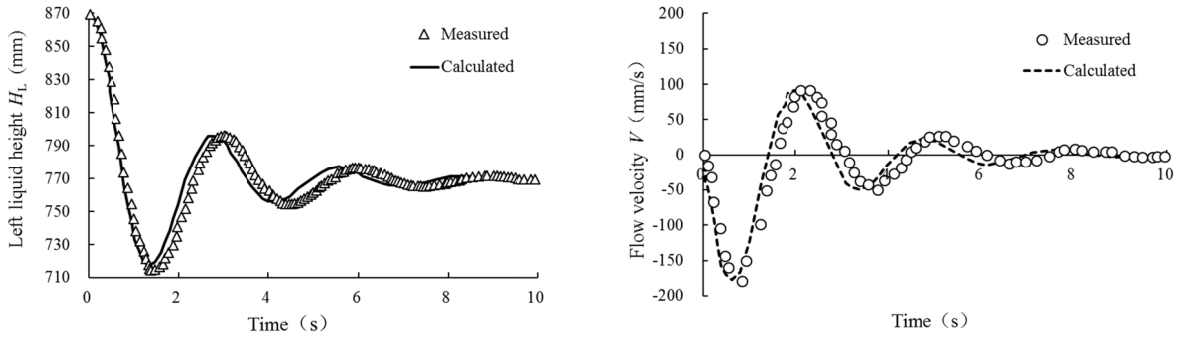

(a) H_L(t) profiles (b) V(t) profiles

Figure 3: Comparison of the calculated results of H_L and V with the experimental results for the 68% glycerin solution in water.

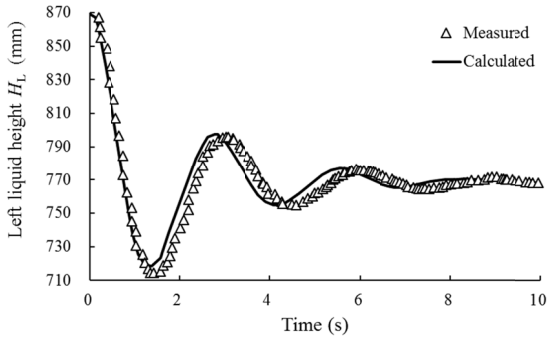

(a) H_L(t) profiles

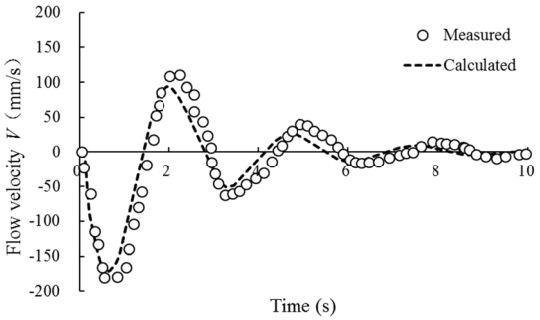

(b) V(t) profiles

Figure 4: Comparison of the calculated results of H_L and V with the experimental results for the 3% acrylic co-polymer solution in water

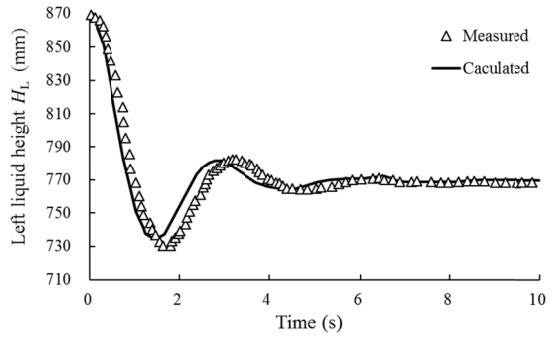

(a) H_L(t) profiles

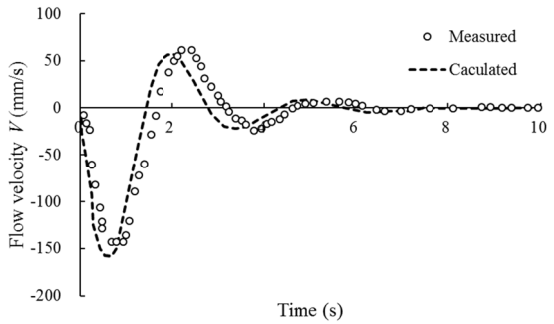

(b) V(t) profiles

Figure 5: Comparison of the experimental results of H_L and V with the calculated results for the 1.8% acrylic co-polymer solution in water.

Table 2: Error of calculated data by the model for 3 non-Newtonian fluid flow experiments.

Fluid Type	Average error of left-liquid height $\bar{E}_{H_L}$	Average error of flow velocity $\bar{E}_V$
68% glycerin solution	1.7%	1.53%
1.8% acrylic co-polymer	2.21%	3.56%
3% acrylic co-polymer	2.3%	2.97%

Case Study

A deep water well in the Gulf of Mexico is used as an example to analyze the unsteady flow for the CMC drilling system. The well data are shown in Table 3. These data were used to calculate the mud flow velocity and mud level in the annulus after a circulation break.

Figure 6 shows the transient flow velocity in the annulus with time after the surface pump is shut down. At the beginning, the mud circulation loses its main power source (i.e., the SPP) due to the shut-down of surface pump, therefore, the mudflow velocity decreases rapidly. When the SPP reaches zero, the maximum mud free-fall velocity in the drill string is reached at point A. After that the mudflow velocity continues to decrease linearly. At point B, the flow pattern transitions from turbulent to laminar flow inside the drill string. Subsequently, the mudflow velocity drops exponentially to zero. Unlike the flow condition in the experiment, the mud column in the drill string does not oscillate because the high-friction pressure loss in the CMC drilling system prevents the surge. The model can also predict the time to reach the mud level equilibrium between in drill string and annulus. When the mudflow velocity drops to zero, the equilibrium is reached. As can be seen from Figure 6, the equilibrium time is 35 minutes. Figure 7 shows the corresponding mud level in the annulus measured from the sea level versus time. As expected, the mud level in the annulus increases rapidly at the beginning and then gradually reaches its final equilibrium position.

Table 3: Basic parameter values.

Parameter	Value
Mud density, g/cm^3	1.50
Seawater density, g/cm^3	1.03
Fluid model	Power-law
Water depth, m	2500
Plastic viscosity, cP	45
Bingham yield point, Pa	0.87
Number of bit nozzles	3
Bit nozzle diameter, 1/32nd in	14
Well vertical depth, m	5000
Length of drill collars, m	91.5
Inner diameter of the last casing, m	0.22289
Open hole diameter, m	0.22225
OD and ID of drill string, m	0.127×0.1086
OD and ID of drill collars, m	0.1778×0.0762
ID of return line, m	0.1524

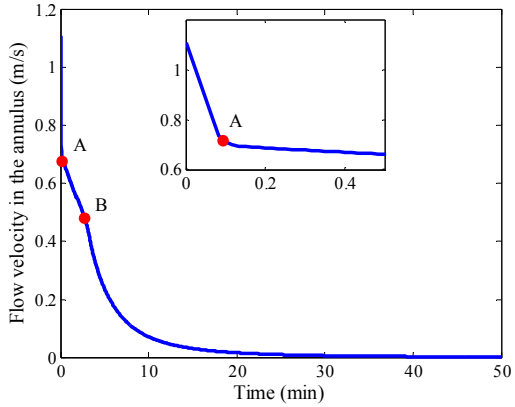

Figure 6: Change of annulus flow velocity over time after the surface pump is shut down

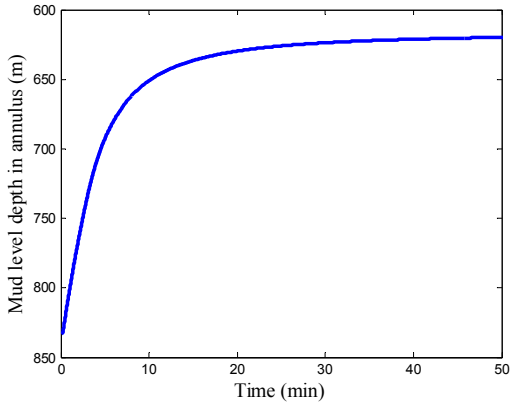

Figure 7: Change of mud level in annulus over time after the surface pump is shut down

The BHP can be predicted based on the mudflow velocity and mud level in the annulus (Figure 8).

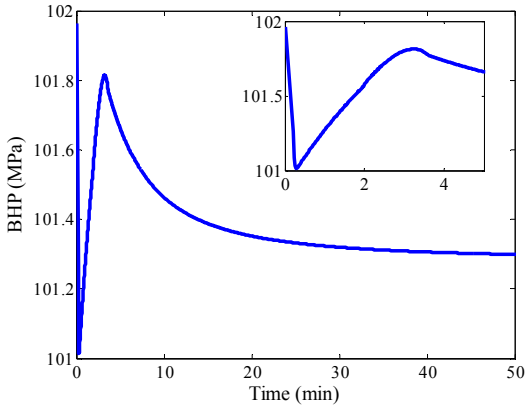

Figure 8: Transient BHP after the surface pump is shut down.

The BHP is the sum of the hydrostatic pressure and friction pressure loss in the annulus. During unsteady flow, a fluctuation in the BHP can occur. Fig. 8 shows that the BHP rapidly decreases within the first few seconds due to the disappearance of the SPP. Subsequently, the BHP increases as the increase in the pressure resulting from the rising mud level in the annulus is larger than the decrease in the pressure caused by reduced annulus flow velocity; when these two equal to each other, the BHP reaches to a new high point; and then the increase in the pressure resulting from the rising mud level in the annulus becomes less than the decrease in the pressure caused by reduced annulus flow velocity, and the BHP decreases gradually and tends to a constant. The fluctuation in the BHP can threaten drilling safety as it can lead to the occurrence of kick.

Applications

Under normal circulation conditions in CMC drilling, the SPP is non-zero, a kick can be detected

by comparing surface pump rate and subsea pump rate. However, detecting kick after the surface pump is shut down is very difficult. The kick is easily masked by the continuous returning flow in the annulus. The normal kick detection method for CMC drilling requires a waiting period for circulation to cease before detecting flow within the well as an indicator of kick. Therefore, the detection of kick is associated with a delay and risks a loss of well control.

However, the timely detection of kick after every pump shutdown is crucial. The above model can provide the transient mudflow characteristics in the annulus after the surface pump is shut down. If the system is coupled to a reservoir productivity model, given by Eq. (8). The unsteady flow of kick after a circulation break can be simulated.

$$q = PI(P_p - P_b) \tag{8}$$

When the kick occurs, the governing equation for the liquid flow velocity in the annulus is as follow:

$$\frac{\partial U_{Ann}}{\partial t} = -\frac{(U_{Ann} - \frac{q}{A_{Ann}})^2 - U_{DC}^2}{2(L_{Ann} + \frac{A_{Ann}}{A_{DC}} L_{DC})} - \frac{(P_{DC,0} - P_{Ann,0}) + (P_{f,DC} + P_{f,Ann} + P_{bit})}{\rho(L_{Ann} + \frac{A_{Ann}}{A_{DC}} L_{DC})} + \frac{(L_{DC} - L_{Ann})g}{(L_{Ann} + \frac{A_{Ann}}{A_{DC}} L_{DC})} + \frac{L_{DC}}{(A_{DC} L_{Ann} + A_{Ann} L_{DC})} \frac{\partial q}{\partial t} \tag{9}$$

In this paper, the emphasis is laid upon analyzing the unsteady flow behavior of the pure liquid phase. The detailed derivation of Eq. (9) is not presented here. The equation just applied in the situation of small kick. For large kick, the fluid in the annulus is transformed from single phase into two-phase. The application of steady friction factor cannot meet the accuracy requirements. The frictional pressure loss of two-phase flow need to be introduced into the equation.

The simulation results are shown in Figure 9 and Figure 10. At the beginning, the BHP is higher than formation pressure, and there is no kick. When the BHP is lower than the formation pressure, formation fluid will invade into the wellbore. The unsteady flow of kick starts to be different from that of no kick. The flow velocity and mud level in annulus of kick are higher than those of no kick, as shown in Fig. 9 and Fig. 10. The model can be used to detect kick and loss of circulation during unsteady flow by comparing the real-time monitored trend with the calculated trend. If real-time monitored flow velocity and mud level in annulus are higher than the calculated trend, a kick is indicated. Conversely, a loss of circulation is indicated. This method can be used to detect kick and loss of circulation in a timely manner during unsteady flow and helps drillers take measures to prevent kick or loss of circulation from developing further in the well. A change in the hook load may be adopted to determine whether a kick or loss of circulation has occurred. However, the technique needs to be further investigated and developed.

The model is also applied to other managed pressure drilling systems, such as constant bottom hole pressure, but needs to be tuned with friction pressure losses.

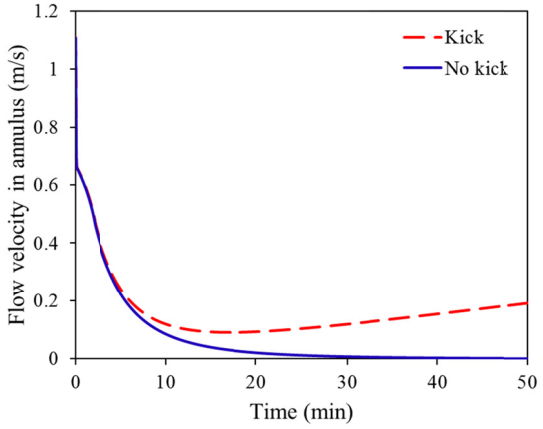

Figure 9: Comparison of annulus flow velocity with and without a kick.

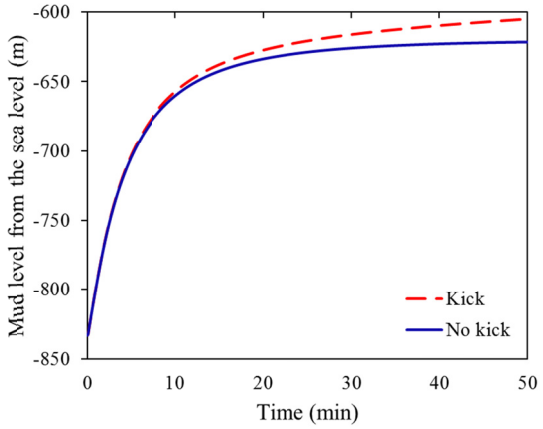

Figure 10: Comparison of annulus mud level with and without a kick.

The drilling fluid has a gelling effect. The transient gelling effect of low-velocity mud in the CMC drilling system has not been considered in this mathematical model. After a circulation break, the subsequent flow is unsteady flow, which means that caution must be exercised to calculate the friction pressure loss. For the CMC drilling system, long mudflow lengths in combination with small fluid acceleration make the application of steady friction factors adequate for friction pressure loss. But for large acceleration of mud, the steady friction factors can be insufficient. Unsteady friction factors need to be introduced into the model to replace the steady friction factors.

SENSITIVITY ANALYSIS

The transient flow inside the drill string and annulus during unsteady flow are influenced by many parameters, including the drill string, well geometry, bit nozzle size, water depth, physical properties of the mud, etc. To understand how these parameters affect flow behavior, a sensitivity analysis was performed for each of these parameters while maintaining the other parameters constant.

(1) Water Depth

The annulus flow velocity and BHP were computed for water depths of 500 m, 1500 m, 2500 m, 3500 m and 4500 m. Figure 11 presents the calculated transient flow velocity of mud in the annulus and BHP for different water depths. As shown in Fig. 11 (a), the flow velocity and equilibrium time directly correlate with the water depth because deeper water generates a greater pressure difference between the inside of the drill string and annulus, which consequently increases the mudflow into the annulus from the drill string after a circulation break. As indicated in Fig. 11 (b), the BHP level drops with water depth for a given well depth. A critical water depth that does not create a fluctuation in the BHP can be determined. At this water depth, the disappearance of the friction pressure loss is compensated completely by the increase in the mud level in the annulus. The final equilibrium BHP is equal to the BHP during circulation. If the water depth exceeds the critical depth, the final equilibrium BHP will directly correlate with the water depth and can exceed the BHP prior to the circulation break, which may result in a loss of circulation. If the water depth is less than the critical depth, the final BHP will decrease as the water depth decreases, which may lead to well kick. Therefore, a fluctuation in the BHP during narrow-margin pressure drilling is a threat to drilling operations.

(2) Mud Density

The annulus flow velocity and BHP were sensitized to mud densities of 1.3 g/cm^3, 1.4 g/cm^3, 1.5 g/cm^3, 1.6 g/cm^3 and 1.7 g/cm^3. As shown in Fig. 12 (a), increases in the mud density will increase the flow velocity due to a greater pressure difference between the inside of the drill string and the annulus. Fig. 12 (b) demonstrates that the mud density also affects the fluctuation in the BHP during the unsteady flow. Again, a critical mud density that does not create fluctuations in the BHP can be identified.

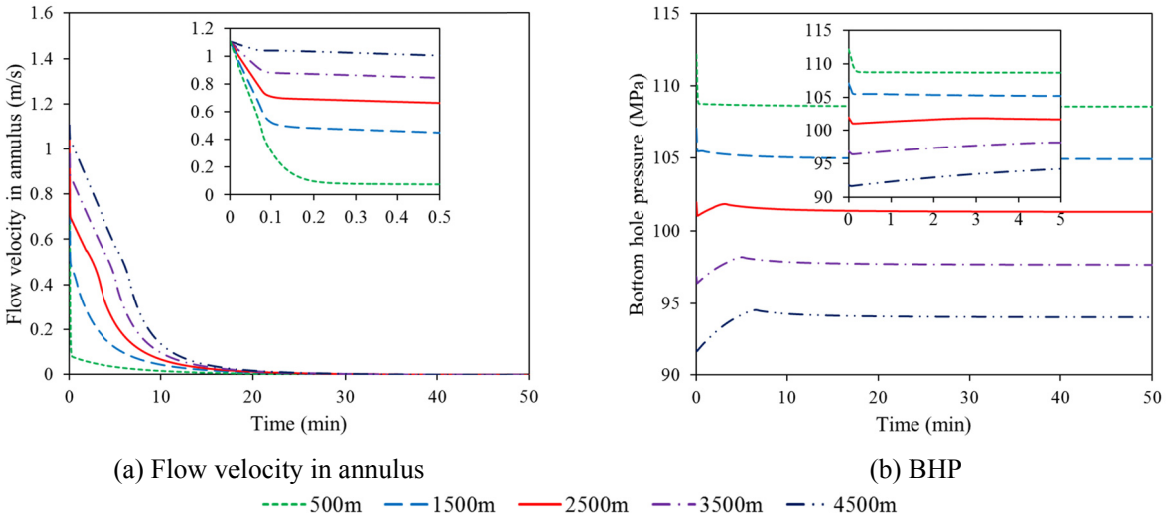

(a) Flow velocity in annulus (b) BHP

Figure 11: Changes of flow velocity in annulus and BHP over time for different water depths.

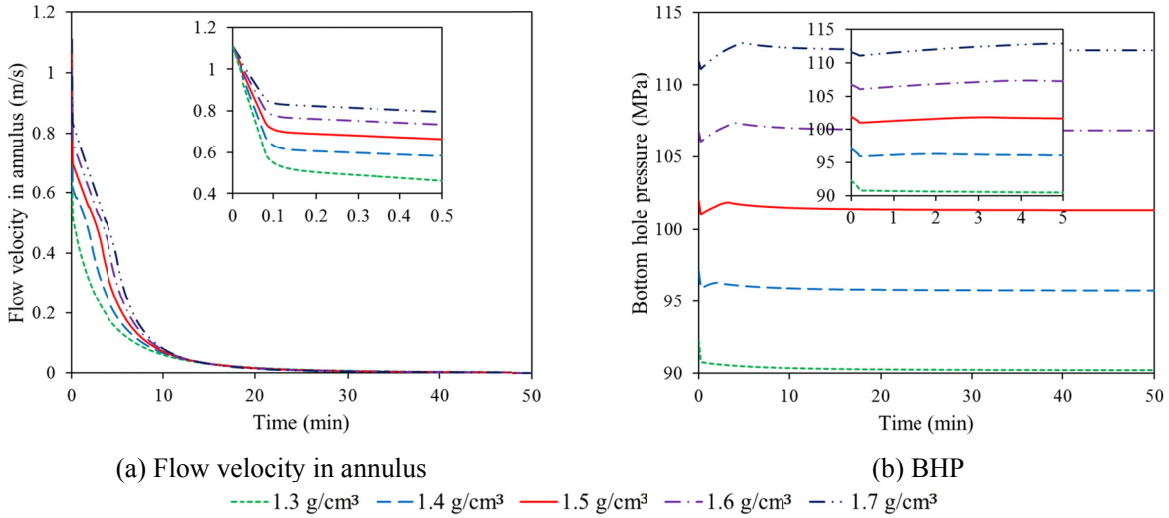

(a) Flow velocity in annulus (b) BHP

Figure 12: Changes of flow velocity in annulus and BHP over time for the different mud densities.

At the critical density, the decrease in annulus friction pressure loss is offset by the increase in the mud level in the annulus. If the mud density exceeds the critical density, the final BHP will exceed the initial BHP while circulating as mud density increases. If the mud density is less than the critical density, the stabilized BHP will be less than the initial BHP as mud density decreases.

(3) Well Depth

The calculated annulus flow velocities and BHPs for well depths of 5500 m, 6500 m, 7500 m, 8500 m and 9500 m are shown in Figure 13. As indicated in Fig. 13 (a), increases in the well depth decrease the rate at which mudflow velocity in the annulus decreases, which prolongs the time required to reach equilibrium. This phenomenon occurs because the friction pressure loss directly correlates with the well depth. Fig. 13 (b) shows that the well depth directly correlates with the BHP, which also affects the pressure fluctuation. Again, a critical well depth that does not result in fluctuations of the BHP can be identified. If the well depth exceeds the critical depth, the stabilized BHP will be less than the initial BHP as well deepens. If the well depth is less than the critical depth, the final BHP will exceed the initial BHP as the well depth decreases.

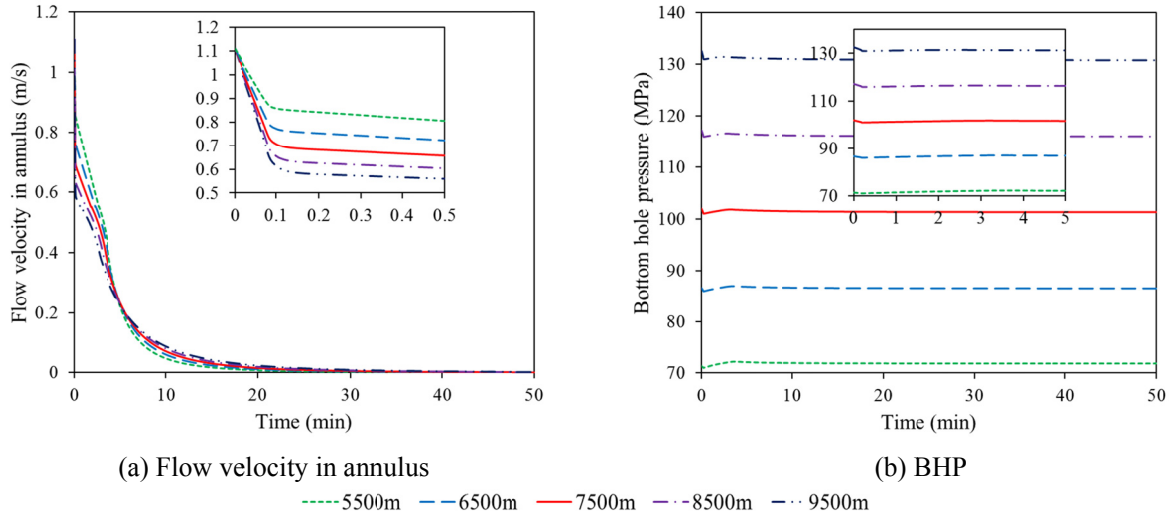

(a) Flow velocity in annulus (b) BHP

Figure 13: Changes in the flow velocity in annulus and BHP over time for different well depths.

(4) Mud Viscosity

The annulus flow velocity and BHP were investigated at mud viscosities of 35 mPa·s, 40 mPa·s, 45 mPa·s, 50 mPa·s and 55 mPa·s. Figure 14 shows transient flow velocity in the annulus and the BHP for different mud viscosities. As indicated in Fig. 14 (a), the mud viscosity affects the flow velocity and the time to reach equilibrium in a complex manner. Generally, a high viscosity will yield a slower decrease in the flow velocity and a longer time to reach equilibrium. As shown in Fig. 14 (b), a higher mud viscosity will reduce the fluctuation in the BHP.

(5) Drill String Size

The calculated annulus flow velocities and BHPs for drill string IDs of 82.5 mm, 93.2 mm, 107.4 mm, 119.5 mm and 130.5 mm are shown in Figure 15(a) and Figure 15(b), respectively. As shown in Fig. 15 (a), the drill string size significantly impacts the mud flow velocity in the annulus and the time to reach equilibrium. For a given wellbore ID, the cross-sectional area of the drill string inversely correlates with the annulus cross-sectional area. For the same volumetric flow rate conditions, a larger drill string ID generates a higher initial flow velocity in the annulus. Increasing the drill string ID decreases the friction pressure loss inside the drill string and increases the annulus frictional pressure loss. Because the friction pressure loss inside the drill string plays a dominant role in the total friction pressure loss, a larger drill string ID will generate a higher flow velocity in the annulus. As revealed in Fig. 15 (b), increasing the drill string ID results increases the equilibrium BHP, because the cross-sectional area of the annulus inversely correlates with the drill string ID; therefore, more mud will flow into the annulus from the drill string. The BHP shows similar trends for different drill string sizes during the unsteady flow. The drill string size does not significantly influence the fluctuation in the BHP.

(6) Nozzle Size

The annulus flow velocity and BHP were sensitized to nozzle sizes of $10/32^{nd}$ in, $12/32^{nd}$ in, $14/32^{nd}$ in, $16/32^{nd}$ in, and $18/32^{nd}$ in. The results of this analysis are presented in Figure 16 (a) and Figure 16 (b). As displayed in Fig. 16 (a), a larger nozzle size normally leads to a fast flow velocity and flow decline, resulting in a shorter time to reach the equilibrium. As indicated in Fig. 16 (b), an increase in the nozzle size typically increases the BHP fluctuation during unsteady flow, but this increase does not significantly affect the final BHP.

(7) Volumetric Flow Rate

The calculated annulus flow velocity and BHP were sensitized to volumetric flow rates of 20 L/s, 25 L/s, 30 L/s, 35 L/s and 40 L/s. As shown in Figure 17, for the same drill string geometry, a different initial circulation rate does not cause noticeable difference of transient mud flow velocity in the annulus and total time for equilibrium except for the first couple of seconds after the surface pump is shut down, and the annulus mud flow velocity rapidly drop to 0.68 m/s for different initial volumetric flow rate. As discussed in the previous section, this phenomenon occurs because the mud flow is powered by the pressure imbalance between the inside of the drill string and the annulus, and the annular flow velocity of 0.68 m/s indicates zero SPP which means a maximum free fall velocity inside the drill string for given system in Table 3.

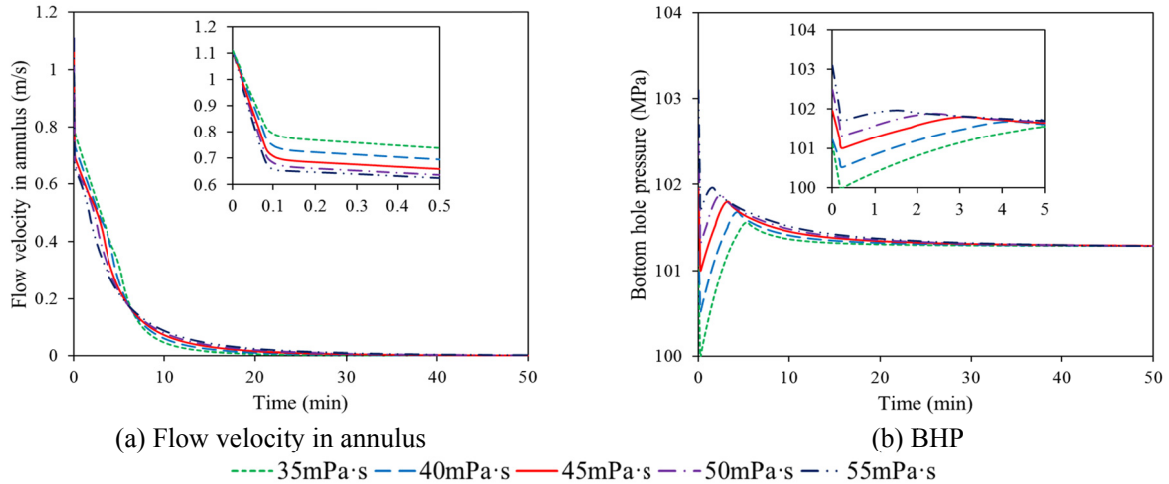

(a) Flow velocity in annulus (b) BHP

Figure 14: Changes in the flow velocity in the annulus and BHP over time for the different mud viscosities.

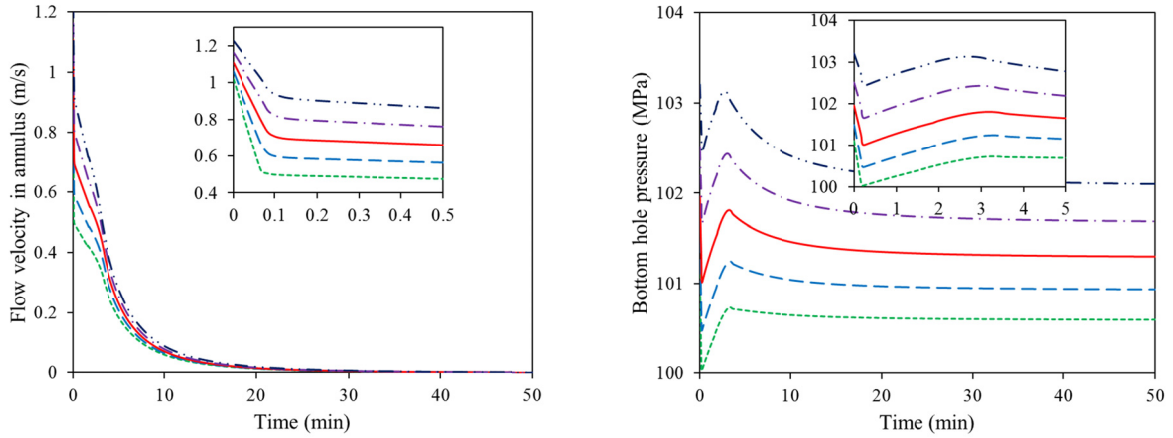

(a) Flow velocity in annulus (b) BHP

Figure 15: Changes in flow velocity in the annulus and BHP over time for the different drill string sizes

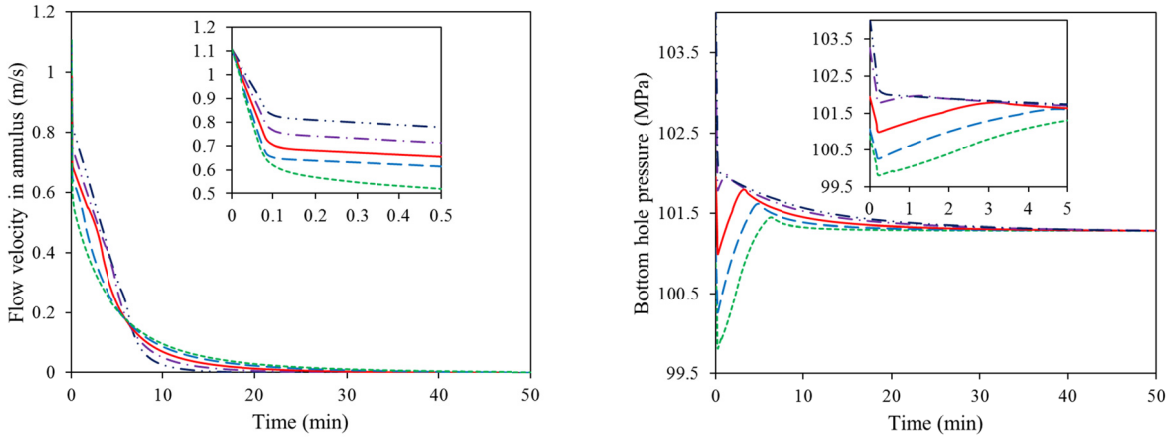

(a) Flow velocity in annulus (b) BHP

Figure 16: Changes in the flow velocity in the annulus and BHP over time for different nozzle sizes.

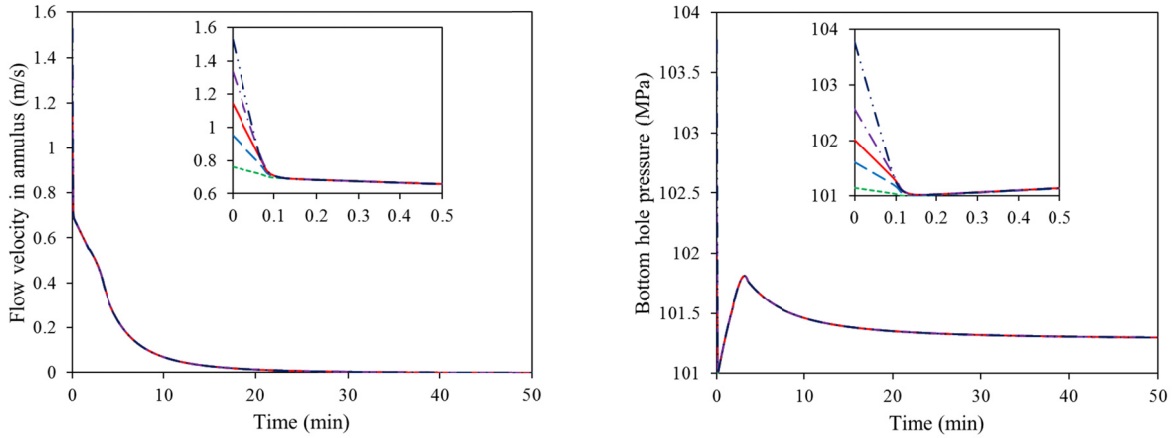

(a) Flow velocity in annulus (b) BHP

Figure 17: Changes in the flow velocity in the annulus and BHP over time for different volumetric flow rates.

CONCLUSIONS

A new mathematical model for the unsteady flow during CMC drilling was developed in this study to simulate the annular after-flow and BHP after a circulation break. The following conclusions are drawn:

1. The mathematical model was verified using experimental obtained from U-tube flow. This verification indicated that the model is accurate, with a maximum average error of 3.56% for the flow velocity.

2. Based on the new mathematical model, a method of early kick detection during the unsteady flow was formulated. This method identifies abnormalities in the mudflow by comparing the model-calculated and measured return flow in the annulus. If the real-time measured flow trend differs from the model-calculated trend, a kick or loss of circulation can be detected in time. This approach will help to overcome the current difficulty of early kick detection during the connection of pipes. Accordingly, drillers can take well control actions in a timely manner to prevent well blowout.

3. Sensitivity analysis of various parameters indicate that the velocity of continuous flow in the annulus is directly proportional to the water depth, mud density, drill string size, and nozzle size and inversely proportional to the well depth and mud viscosity. The time required for the unsteady flow to reach equilibrium is directly proportional to the water depth, well depth, mud density, mud viscosity, drill string size and inversely proportional to the nozzle size.

4. The water depth, mud density and drill string size were identified to be three major factors affecting the fluctuation in the BHP after a circulation break. Whereas the water depth cannot be controlled, the mud density and drill string size should be carefully selected to minimize the risk of well blowout.

ACKNOWLEDGMENT

The authors wish to acknowledge the Key Program of National Natural Science Foundation of China (Contract No. 51334003 and 51434009) for the financial support.

NOMENCLATURE

A_{Ann}	Cross-sectional area of annulus (m^2)
A_{DC}	Cross-sectional area of drill string (m^2)
G	Gravitational acceleration (m/s^2)
H_{L}	Left-liquid height (mm)
H_{R}	Right-liquid height (mm)
h_{w}	Water depth (m)
ID	Inner diameter
L_{Ann}	Length of mud column in the annulus (m)
L_{DC}	Length of mud column inside the drill string (m)
L_{well}	Well depth below the Kelly bushing (m)
N	Time node
OD	Outside diameter
$P_{\text{Ann, 0}}$	Boundary pressure of mud level in the annulus (Pa)
P_b	Bottom hole pressure (Pa)
P_{bit}	Friction pressure loss in drill bit (Pa)
$P_{\text{DC, 0}}$	Boundary pressure of mud level inside the drilling string (Pa)
$P_{f,\text{ Ann}}$	Friction pressure loss in the annulus (Pa)
$P_{f,\text{ DC, 0}}$	Friction pressure loss in the drill string (Pa)
PI	Productivity index ($m^3/(Pa \cdot s)$)
P_p	Pore pressure (Pa)
Q	Reservoir inflow rate (m^3/s)
U_0	Mud flow velocity in drill string before the surface pump is shut down (m/s)
U_{Ann}	Average flow velocity of fluid in the annulus (m/s)
U_{DC}	Average flow velocity of fluid inside the drill string (m/s)
ρ	Density of mud (kg/m^3)
ρ_{w}	Seawater density (kg/m^3)
Δt	Unit time step (s)

REFERENCES

Børre, F. and Sigbjørn, S., Controlled mud-cap drilling for subsea applications: Well-control challenges in deep water. SPE Drilling & Completion, 21(2), 133-140 (2006).

Choe, J. and Juvkam-Wold, H. C., Well control aspects of riserless drilling. SPE Annual Technical Conference and Exhibition, Society of Petroleum Engineers. New Orleans, Louisiana (1998).

Choe, J., Analysis of riserless drilling and well-control hydraulics. SPE Drilling & Completion, 14(1), 71-81(1999).

Choe, J., Schubert, J. J. and Juvkam-Wold, H. C., Analyses and procedures for kick detection in subsea mud-lift drilling. SPE Drilling & Completion, 22(4), 296-303 (2007).

Børre, F. and Stave, R., Drilling depleted reservoirs using controlled mud level technology in mature subsea fields. SPE Bergen One Day Seminar, Bergen, Norway (2014).

Godhavn, J. M., Hauge, E., Molde, D. O., Kjøsnes, I., Gaassand, S., Fossli, S. B., Stave, R., ECD Man-

agement Toolbox for Floating Drilling Units. Offshore Technology Conference, Houston, Texas (2014).
JPT Staff, EC-drill eliminates effect of equivalent circulating density. Journal of Petroleum Technology, 65(8), 38-40 (2013).
Malt, R., and Stave, R., EC-drill MPD dual gradient drilling for challenging pressure regimes. Offshore Technology Conference-Asia, Kuala Lumpur, Malaysia (2014).
Ochoa, M. V., Analysis of Drilling Fluid Rheology and Tool Joint Effect to Reduce Errors in Hydraulics Calculations. Ph.D. Thesis, Texas A&M University (2006).
Ogawa, A., Tokiwa, S., Mutou, M., Mogi, K., Sugawara, T., Watanabe, M., Satou, K., Kikawada, T., Shishido, K., Matumoto, N., Damped oscillation of liquid column in vertical U-tube for Newtonian and non-Newtonian liquids. Journal of Thermal Science, 16(4), 289-300 (2007).
Sauer, C. W., Mud displacement during cementing: A state of the art. Journal of Petroleum Technology, 39(9), 1091-1101 (1987).
Schubert, J. J. and Juvkam-world, H. C., Well-control procedures for dual-gradient drilling as compared to conventional riser drilling. SPE Drilling & Completion, 21(04), 287-295 (2006).
Shaughnessy, J. M., Armagost, W. K., Herrmann, R. P., Problems of Ultra-deepwater drilling. SPE/IADC Drilling Conference, Amsterdam, Netherlands (1999).
Shaughnessy, J. M., Daugherty, W. T., Graff, R. L., Durkee, T., More ultra-deepwater drilling problems. SPE/IADC Drilling Conference, Amsterdam, The Netherlands (2007).
Stave, R., Implementation of dual gradient drilling. Offshore Technology Conference, Houston, Texas (2014).
Bewley, T. R., Numerical Renaissance, Advance Copy. Renaissance Press, La Jolla (2012).
Çengel, Y. A. and Cimbala, J. M., Fluid Mechanics: Fundamentals and Applications. McGraw Hill Higher Education, America (2010).
Ziegler, R., Dual gradient drilling is ready for prime-time: The benefits of a retrofit system for better well control, enhanced water depth capability and flat time reduction. Offshore Technology Conference, Houston, Texas (2014).

APPENDIX A: Derivation Process for Governing Equation

In order to develop the mathematical model to describe the transient flow characteristic in the annulus after surface pump shutdown, the following assumptions were made: 1) all pumps involved are stopped immediately; 2) the drill string is disconnected from the surface pumps and open at the surface; 3) the mud is incompressible; 4) the cross-sectional areas inside the drill string and annulus are constant; 5) the flow is one-dimensional; 6) the mud density is constant; 7) the mud does not gel; and 8) the well is isothermal.

The well hole can be divided into two parts, the drill string and the annulus. The mud flows from the drill string into the annulus, and this direction was defined as positive. Figure A1 shows the mudflow in the wellbore at any time during the unsteady flow. First, the drill string was studied as a control volume; the upper and lower boundaries of the control volume are B1 and B2, respectively. Because the fluid level in drill string is continuously changing, the control volume can be regarded as a deforming control volume.

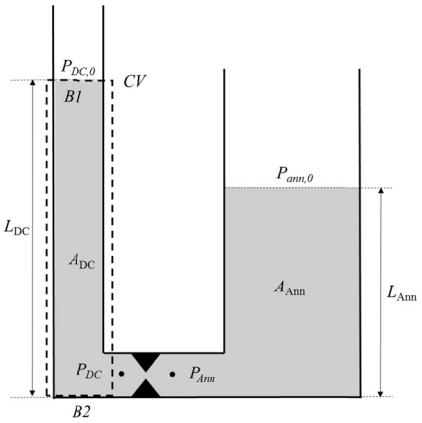

Figure A1: Illustration of mudflow in the wellbore at any time during the unsteady flow.

For this situation, the Reynolds transport theorem is expressed as follows (Çengel and Cimbala, 2010):

$$\frac{d}{dt}\int_{CV} B dV = \int_{CV} \frac{\partial B}{\partial t} dV + \int_{CS} B(\mathbf{V} - \mathbf{V}_{CS}) \cdot \mathbf{n} dA$$

where B can represent several parameters per unit volume, such as the mass, momentum or energy; $\mathbf{V}$ is the local material velocity; $\mathbf{V}_{CS}$ is the local con-

trol surface velocity at the surface element dA; $\mathbf{n}$ represents the outward-pointing unit normal vector associated with dA; CV denotes the control volume; CS represents the surface area of the control volume.

According to the Reynolds transport theorem of a deforming control volume, the mass balance equation for the drill string can be written as follows:

$$\rho A_{DC}\frac{\partial(L_{DC})}{\partial t}+\rho A_{DC}(U_{DC}-U_{B2})=0 \tag{A1}$$

The momentum balance equation for the annulus can be written as follows:

$$\frac{\partial(\rho A_{DC}L_{DC}U_{DC})}{\partial t}+\rho A_{DC}U_{DC}(U_{DC}-U_{B2})= -\Delta P A_{DC}-P_{f,DC}A_{DC}+\rho L_{DC}A_{DC}g \tag{A2}$$

where ρ is the density of the mud in kg/m^3; A_{DC} is the cross-sectional area of the drill string in m^2; U_{DC} is the fluid velocity in the drill string in m/s; L_{DC} is the length from the bottom to the fluid level in the drill string in m; U_{B2} is the average velocity of the lower boundary of the control volume in m/s (when the lower boundary is fixed, the velocity is 0 m/s); $P_{f,\mathrm{DC}}$ is the friction pressure loss in the drill string in Pa; g is the gravitational acceleration in m/s^2. ΔP is the pressure difference between two boundaries of the control volume in Pa ($\Delta P=P_{B2}-P_{B1}$, $P_{B1}=P_{DC,0}$); $P_{DC,0}$ is the atmospheric pressure in Pa because the drill string is open at the surface after the surface pump is shut down ($P_{B2}=P_{DC}$); and P_{DC} is the bottom hole pressure in the drill string in Pa.

Expanding the time derivative of the momentum balance equation and combining Equations (A1) and (A2) yields the following expression for the momentum balance equation of the drill string:

$$L_{DC}\frac{\partial U_{DC}}{\partial t}=-\frac{P_{\mathrm{DC}}-P_{DC,0}}{\rho}-\frac{P_{f,DC}}{\rho}+L_{DC}g \tag{A3}$$

Similarly, the momentum balance equation for the annulus can also be obtained:

$$L_{Ann}\frac{\partial U_{Ann}}{\partial t}=-\frac{P_{Ann,0}-P_{Ann}}{\rho}-\frac{P_{f,Ann}}{\rho}-L_{Ann}g \tag{A4}$$

where L_{Ann} is the length from the bottom to the fluid level in the annulus in m; U_{Ann} is the average flow velocity of the fluid in the annulus in m/s; $P_{Ann,\,0}$ is the atmospheric pressure because the annulus is open at the surface. P_{Ann} is the bottom hole pressure in the annulus in Pa; $P_{f,Ann}$ is the friction pressure loss in the annulus in Pa.

Combining the drill string and annulus momentum balance Equations, (A3) and (A4), yields the following expression for the momentum balance equation for the fluid in the entire well:

$$L_{Ann}\frac{\partial U_{Ann}}{\partial t}+L_{DC}\frac{\partial U_{DC}}{\partial t}= -\frac{P_{\mathrm{DC}}-P_{Ann}}{\rho}-\frac{P_{DC,0}-P_{Ann,0}}{\rho} -\left(\frac{P_{f,DC}}{\rho}+\frac{P_{f,Ann}}{\rho}\right)+(L_{DC}-L_{Ann})g \tag{A5}$$

The wellbore mud is incompressible; therefore, the volumetric flow is conserved, which implies that the rate of volumetric change over time is the same inside the drill string and the annulus:

$$A_{DC}\frac{\partial U_{DC}}{\partial t}=A_{Ann}\frac{\partial U_{Ann}}{\partial t} \tag{A6}$$

According to the energy balance equation, the following formula can be obtained:

$$\frac{P_{DC}}{\rho}+\frac{U_{DC}^2}{2}=\frac{P_{Ann}}{\rho}+\frac{U_{Ann}^2}{2}+\frac{P_{bit}}{\rho} \tag{A7}$$

where A_{Ann} is the cross-sectional area of annulus in m^2; P_{bit} is the friction pressure loss in the drill bit in Pa. The friction pressure loss calculation is well established, and the detailed method used to calculate $P_{f,DC}$, $P_{f,Ann}$ and P_{bit} can be obtained from the literature (Ochoa, 2006).

According to Equations (A5) (A6) (A7), U_{DC} is eliminated, and the equation governing the liquid flow velocity in the annulus can be derived as follows:

$$\frac{\partial U_{Ann}}{\partial t}=-\frac{U_{Ann}^2-U_{DC}^2}{2(L_{Ann}+\frac{A_{Ann}}{A_{DC}}L_{DC})}-\frac{P_{DC,0}-P_{Ann,0}}{\rho(L_{Ann}+\frac{A_{Ann}}{A_{DC}}L_{DC})} -\frac{P_{f,DC}+P_{f,Ann}+P_{bit}}{\rho(L_{Ann}+\frac{A_{Ann}}{A_{DC}}L_{DC})}+\frac{(L_{DC}-L_{Ann})g}{(L_{Ann}+\frac{A_{Ann}}{A_{DC}}L_{DC})} \tag{A8}$$

Thus, the final expression for the motion equation for the length of mud column L_{Ann} in the annulus can be obtained:

$$\frac{\partial L_{Ann}}{\partial t}=-U_{Ann} \tag{A9}$$